ELSEVIER

Solid State Ionics 133 (2000) 79–97

SOLID STATE IONICS

www.elsevier.com/locate/ssi

Comparison of the universal dynamic response power-law fitting model for conducting systems with superior alternative models

J. Ross Macdonald*

Department of Physics and Astronomy, University of North Carolina, Chapel Hill, NC 27599-3255, USA

Received 11 October 1999; received in revised form 5 June 2000; accepted 13 June 2000

Abstract

For at least 5 years there has been considerable controversy concerning the relative value of power-law and electric modulus formalism models for fitting and interpreting dispersed frequency-response data for ionically conducting glasses, melts, and other disordered solids. Conclusions of various authors have ranged from preferring one or the other to neither. Here, detailed complex-nonlinear-least-squares fitting of data for a trisilicate glass with several different dispersion models leads to the conclusion that 'neither' of the above is the correct conclusion for an adequate analysis of bulk-material behavior in this and other materials. The power-law model is nonphysical, and the usual modulus formalism approach is faulty in two different ways. For the near-room-temperature data set analyzed here, it was found that when electrode effects were included in a composite fitting model, they contributed significantly to high-, but not low-frequency response. Their presence may explain the increasing log–log slope of the real part of the conductivity with increasing frequency found for many materials. The corrected modulus formalism approach, involving a Kohlrausch–Williams–Watts model, the KWW1, was found to be the best of those used to represent bulk response. Contrary to common expectation, the original modulus formalism and KWW1 models do not lead to stretched-exponential response in the time domain. Best fitting required not only a model for bulk response but one for electrode response as well and necessarily also involved a separate fitting parameter to account for high-frequency-limiting dipolar dielectric effects.

Keywords: Conductivity relaxation; Disordered materials; Electric modulus formalism; Electrode effects; Impedance spectroscopy; Ionic glasses; Kohlrausch–Williams–Watts; Power law; Universal dynamic response

1. Introduction and background

Much effort has been applied for many years toward understanding processes that lead to dispersion in electrical and mechanical small-signal frequency and temporal response. In pursuit of this goal, many dispersion models have been developed, although none of them is fully based on many-body microscopic physical processes and on analysis which leads, for example, to temperature-dependence relations for all of the model parameters. Richard Feynman said, ''Experiment is the sole judge of scientific truth''. In the present state of our knowledge of dispersion processes in solids and the

*Tel.: +1-919-967-5005; fax: +1-919-962-0480.
E-mail address: macd@email.unc.edu (J.R. Macdonald).

0167-2738/00/$ – see front matter
PII: S0167-2738(00)00737-2

interactions leading to them, it is thus particularly important to find ways to analyze experimental data that allow simultaneously present processes to be separated and each process examined in detail. Adequate and appropriate model fitting is therefore of paramount importance and has not usually been pursued previously in sufficient detail.

The present work discusses and compares the utility of several models that have been used in the past for thermally activated, conductive systems. It describes important fitting criteria and illustrates their application for choosing the most appropriate model for fitting frequency-response data of such systems.

1.1. Conductive-system and dielectric-system dispersion

An important distinction needs to be made at the outset: that between dielectric-system-dispersion (DSD) and conductive-system-dispersion (CSD). See Appendix A for mathematical details and definitions. Although the following discussion is elementary, its conclusions are not always applied. The response of a dielectric system, best modeled at the complex dielectric constant level, $\epsilon(\omega) = \epsilon'(\omega) - i\epsilon''(\omega)$, or associated permittivity level, involves induced or permanent dipoles and may be dispersed (non-Debye). Any dc leakage conductance present is associated with mobile charge, and although it may be thermally activated, it often does not involve dispersed behavior, and its magnitude is essentially unrelated to dipolar electrical response. Even in the absence of dielectric dispersion in the usual immittance-spectroscopy frequency range, dielectric systems always involve a high-frequency-limiting true dielectric constant, ϵ_{D_∞} (>1 for real materials). A list of acronym and symbol definitions is included at the end of this work.

In contrast to a dielectric system, a pure conductive-system solid material involves only the motion of monopoles, such as through ionic hopping. Its response is best modeled at the complex resistivity (or impedance) level, $\rho(\omega) = \rho'(\omega) + i\rho''(\omega) = 1/\sigma(\omega)$, and it usually involves dispersive relaxation. Here the complex conductivity is $\sigma(\omega) = \sigma'(\omega) + i\sigma''(\omega)$. The dc resistivity, $\rho_0 \equiv \rho'(0)$, is usually thermally activated and may sometimes be so large that it cannot be accurately estimated in the longtime or low-frequency region experimentally accessible at low temperatures. Conductive-system dc and ac responses are, unlike the DSD situation, closely related.

Even when the high-frequency limiting resistivity, $\rho_\infty \equiv \rho'(\infty)$, is non-zero, it is often too small to be determined in the accessible frequency range, but experimental frequency-response data always include the non-negligible effect of ϵ_{D_∞}. Thus, while the electrical response of insulating polymers or very-large band-gap crystals may be well approximated by pure DSD, conducting-system response is never pure for real data but always includes non-zero ϵ_{D_∞} effects. Finally, there seem to be some situations where both conductive and dielectric dispersion are simultaneously important in the frequency region of interest; see later discussion. Although we shall deal here primarily with CSD, a general equivalent circuit which may be used to fit data with both CSD and DSD simultaneously present, as well as electrode effects, is shown in Fig. 1. Only those elements of this circuit needed for good fitting of a specific data set are actually used.

1.2. Power-law models and response

There are many misconceptions about power-law frequency-response fitting models, models which have been widely used for many years. One purpose of the present work is to try to clear up some of these misconceptions. Another one is to try to convince practitioners in the field of immittance spectroscopy to eschew the use of power-law response [PLR] models for CSD data fitting over a wide frequency range. This approach has been widely used in the past, at least in part because nearly all dispersed frequency response data, whether arising from dielectric or conductive processes, can be well fitted over a finite but limited frequency range by a power law. In addition, the charmed life of power-law models for fitting has been prolonged by the widespread use of log–log plots, say of the real part of the complex conductivity, $\sigma'(\omega)$, versus frequency, plots that can make adequate visual discrimination between true and approximate PLR impossible, especially when significant errors are present in the data.

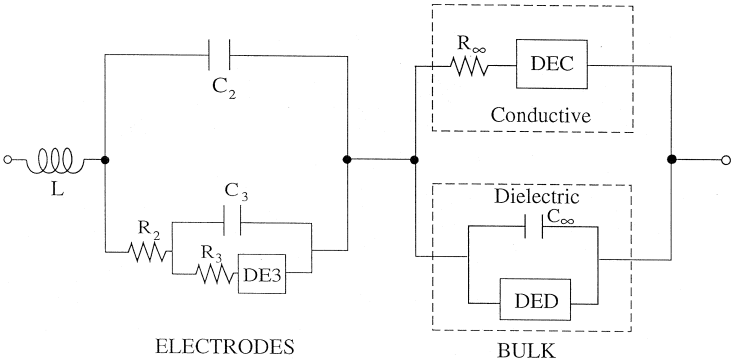

Fig. 1. Circuit used for LEVM fitting of frequency-response data involving both electrode effects and bulk dispersion. Here, the DE3 block may be used to help model electrode response and may represent any distributed circuit element, such as the ZC, that is available in the LEVM program. Further, C_2 may be used to represent a double-layer capacitance. The DEC (distributed-element conductive) block is used for a conductive-system-dispersion model, and the DED one for a dielectric-system-dispersion model. C_∞ is the bulk geometrical capacitance associated with $\epsilon_{D\infty}$, and a conductance G_p (conductivity σ_p), not shown, may also be present, if needed, in parallel with C_∞. LEVM provides many choices for DEC and DED response models.

1.2.1. Forms of universal dynamic response models

First, consider PLR history and nomenclature. Many pertinent references (e.g. [1–12]) credit such response to Jonscher [13–16], who identified it as ‘‘‘Universal’ dielectric response’’, commonly acronymed as UDR. But, in keeping with this designation, Jonscher was nearly exclusively concerned with dielectric systems, ones where dc conductivity, $\sigma_0 \equiv \sigma'(0)$, was rarely included. Thus, Jonscher wrote in [13]

$$\sigma'(\omega) \propto \omega^n \quad n < 1, \tag{1}$$

and although in [14–16] he proposed the expression

$$\sigma'(\omega) = \sigma_0(T) + A(T)\omega^n \tag{2}$$

he did not discuss any explicit relationship between σ_0 and A since none would be expected for a pure dielectric system involving dipoles together with an unrelated leakage conductivity involving mobile charges. Although even earlier [17] Jonscher did list an equation equivalent to (2) as applicable for low-conductivity materials, it was not there identified as UDR.

Later, the acronym UDR was extended to mean ‘Universal dynamic response’ in order for it to include conductive-system behavior, and it became common to write [2–8]

$$\sigma'(\omega) = \sigma_0 + A\omega^n \quad 0 < n < 1, \tag{3}$$

with both σ_0 and A thermally activated. Almond and co-workers [1,18,19] rewrote Eq. (2) in the alternate form

$$\sigma'(\omega) = \sigma_0[1 + (\omega/\omega_p)^n], \tag{4}$$

where the reduced frequency ω_p was identified as an ion hopping rate. This identification was soon shown to be inappropriate [20,21], however. Eq. (4) has also been rewritten for conductive situations in the equivalent form [4,5]

$$\sigma'(\omega) = \sigma_0[1 + (\omega\tau_p)^n], \tag{5}$$

where both σ_0 and τ_p involve equal, or nearly equal, activation energies for conductive (but not for dielectric) situations.

It is incorrect to state, as in, e.g. [1,3–11,22] and elsewhere, that Jonscher proposed Eq. (2) in [13], and it is also misleading to ascribe the terminology ‘universal dynamic response,’ to Jonscher, as done in [2,7,9,10,22,23]. These relatively minor errors, once published, seem to have a life of their own as they continue to be repeated by subsequent authors who evidently do not check the original work. Nevertheless, proper assignment of credit is an important element in science, and even long-standing errors should be corrected.

For PLR with $n < 1$, Eq. (5) should be replaced by the more general and appropriate complex expression

$$\sigma(\omega) = \sigma_0[1 + (i\omega\tau_o)^n] \quad 0 < n < 1, \tag{6}$$

as discussed in detail in [20]. Here $\tau_p = \tau_o[\cos(n\pi/2)]^{1/n}$; τ_o is the more basic quantity; and the model reduces to Debye relaxation (no dispersion) when $n = 1$. It should be noted that Eq. (6) is of the form of the Cole–Cole dielectric response model [24] when that model is defined at the complex resistivity level and then converted to the complex conductivity level. It follows from (6) that

$$\sigma'(\omega) = \sigma_0[1 + (\omega\tau_o)^n \cos(n\pi/2)], \tag{7}$$

a PLR expression that leads to exactly the same fit of a given data set as does Eq. (5), except for a different τ, but not n, estimate. Nevertheless, Eq. (6) is superior to Eq. (5) since (6) includes both a real part and its associated imaginary one in a natural way.

It is worth remarking that a form of Eq. (6) was apparently first proposed for conductive-system data fitting as early as 1957 [25], and was applied for ionic materials in 1973 [26], further reasons for not identifying conductive-system universal dynamic response with Jonscher. For convenience, the complex power-law response model of Eq. (6) will be designated by ZC, reflecting its definition at the impedance level and its connection to Cole–Cole response [27]. The ZC has been used recently in [28] and cited without provenance in [29]. Because the ZC is actually a CSD0 rather than a CSD1 response model (see Appendix A for the distinction), it will be designated by either ZC or ZC0 hereafter, with the latter referring explicitly to the response model of Eq. (6). An equation essentially equivalent to Eq. (6) was derived, independently of the earlier work, in [8] and was based on the assumption of fractional-exponent power-law temporal response. But there is no adequate many-body microscopic analysis available that leads to Eq. (6), and it should be considered empirical for the present.

All PLR equations discussed above are of CSD0 form, but explicit recognition of this by means of 0 subscripts has been mostly suppressed here for simplicity. A full model appropriate for fitting must properly take account of ϵ_{D_∞}. Let us designate such a full model by a subscript 'T' for 'Total,' but treat electrode effects separately if present. Then it follows that we may write for total CSDk response

$$\sigma_{Tk}(\omega) = \{\rho_{Tk}(\omega)\}^{-1} = \sigma_k(\omega) + i\omega\epsilon_V\epsilon_x, \tag{8}$$

where $\sigma_k(\omega)$ is the pure CSDk part of the full model and $k = 0$ or 1. Therefore for the ZC0 model, $\sigma_k(\omega)$ is just the $\sigma(\omega)$ of Eq. (6). Here ϵ_V is the permittivity of vacuum; ϵ_∞ is the full high-frequency-limiting dielectric constant; and the free fitting parameter ϵ_x is ϵ_∞ for models such as the ZC0 which involve no mobile-charge contribution to ϵ_∞, and $\epsilon_x = \epsilon_{D_\infty}$ for those that do, as discussed in Section 2.3.1.

Although the added ϵ_x capacitative term has no effect on fitting real-part conductivity data, it is of great significance for fitting data transformed to other levels, such as the complex modulus one. The CSDk-model modulus, $M_k(\omega)$, is defined as $i\omega\epsilon_V\rho_k(\omega) = 1/\epsilon_k(\omega)$, but the actual modulus, as calculated from experimental $\rho_T(\omega)$ data, is $M(\omega) = i\omega\epsilon_V\rho_T(\omega)$, and it should be compared to $M_{Tk}(\omega) = i\omega\epsilon_V\rho_{Tk}(\omega) = 1/\epsilon_{Tk}(\omega) = 1/\{\epsilon_x + \epsilon_k(\omega)\}$, where $\epsilon_k(\omega)$ is a complex dielectric constant associated entirely with CSD effects, as discussed in Appendix A.

Eq. (6) is made up of the sum of a constant and a PLR *constant-phase element* defined at the complex conductivity level as $B(i\omega)^n$, where B is frequency independent [27,30]. Although the importance of the constant-phase element was emphasized by Jonscher for dielectric response [16,31], it was introduced at least as early as 1932 by Fricke [32], and PLR was demonstrated for conductive systems by Pollak and Geballe in 1961 [33]. Thus, PLR fitting models have a long and varied history, one that suggests that the common usage [5,12] 'Jonscher power law' is inappropriate for conductive-system response.

There is an interesting discontinuity in PLR at $n = 1$. Although Eqs. (5) and (7) can fit the same data equally well for $0 \le n < 1$, this is no longer the case at $n = 1$ since Eq. (5) still involves dispersed response for this value and Eq. (7) does not. Thus, if experimental data can be well fitted over a particular frequency range by Eq. (5) with $n = 1$, one must expect that the associated $\sigma''(\omega)$ response will be different from that of a frequency-independent capacitance. Although the $\sigma''(\omega)$ response associated with that of Eq. (5) when $n \ge 1$ can in principle be calculated by a Kronig–Kramers transformation, low- and high-frequency extrapolation is always

needed to zero and infinite frequencies, respectively, and such a transformation is difficult to implement accurately when the data extend over many decades. It is therefore more appropriate to avoid uncertainties by using only the available data and obtain imaginary-part response from real-part data by first estimating the associated distribution of relaxation times (DRT) from the given data, and then using the result to calculate the associated imaginary part ([27], pp. 181–185, [34–37]). In unpublished work of the author, such calculations have been carried out for exact data with $n = 1$ and 1.3 using the freely available complex-nonlinear-least-squares (CNLS) fitting/inversion computer program LEVM [38,39].

Although Nowick and his co-workers [2,7] have presented PLR data-fitting results that seemingly led to actual $n = 1$ estimated values at low temperatures, termed a 'new universality' [2], it was shown that more detailed and accurate analysis of some of these data, including dielectric-system response and electrode effects as well as bulk conductive-system behavior, did not lead to constant-loss $n = 1$ results but to estimated values close to, but less than unity, ones primarily associated with dielectric effects [9,40–42]. Although n estimates of the order of 1.3 for very high frequencies have been published [43–46], the data tend to be somewhat irregular and little or no associated $\sigma''(\omega)$ values have been presented or discussed. Finally, it is important to recognize that power-law fitting of $\sigma'(\omega)$ data yields an estimate of an exponent n that is a weighted average of the actual, possibly frequency-dependent log–log slope, $s \equiv [\omega/\sigma'(\omega)][d\sigma'(\omega)/d\omega]$, only frequency independent when the data are of exact power-law form and errors are negligible. It is thus important and instructive to calculate $s(\omega)$ for any power-law fit (as in, e.g. [40–42]), particularly for any unusual n estimates that might otherwise suggest some kind of a new universality.

1.2.2. Some PLR-model limitations

There is an intrinsic limitation to the applicability of such response models as the ZC and other PLR models: they involve physically unrealizable response in limiting frequency regions [14,27,35,36]. For example, for the ZC with $n < 1$, the quantity $\Delta\sigma(\omega) \equiv \sigma'(\omega) - \sigma_0$ approaches the slope $s = n$ in the limit of low frequencies instead of the proper limiting slope of 2, and, in addition, Eq. (6) leads to non-realizable continually increasing conductivity $\sigma'(\omega)$ as ω increases indefinitely, except when $n = 1$. Finally, the ZC0 and many other response models do not lead to a temperature-independent distribution of activation energies (DAE) when τ_o is thermally activated [47]. Some possibilities for the temperature dependence of an exponential DAE are discussed in [48].

The above erroneous limiting behaviors are in themselves sufficient reasons why a PLR model should not be used except for preliminary fitting. As we shall see, such a model may be particularly misleading when used to estimate bulk-response values of σ_0 and n. Although many empirical or semi-empirical models do not suffer from this defect, as discussed and demonstrated below, nearly all of them, including the ZC, involve PLR in the limit of high frequencies (see [49] for a detailed discussion of limiting slopes) and thus require modification that leads to Debye response in the high-frequency limit, as in the cutoff approach discussed below.

1.3. The KWW model

A model which has apparently fitted quite well much conductive-system immittance spectroscopy data is the Kohlrausch–Williams–Watts (KWW) one [50,51], which involves a shape parameter β, with $0 < \beta \leq 1$. But few of these fits have involved CNLS, very few have taken electrode effects into account, and, when the modulus formalism approach [MFA] of [52,53] has been used, it has nearly always been incorrectly applied for estimation of β (see, e.g. [5,35,52–56]). The main elements and defects of the MFA are discussed in Appendix A, as well as two different types of general CSD models: CSD0 and CSD1. We shall use the 0 and 1 subscripts to identify them and their parameters. Thus, if the original KWW model is used for describing conductive-system bulk behavior, it is designated KWW0, and involves stretched-exponential temporal response with $\beta = \beta_0$.

The MFA, sometimes called the electric modulus formalism, is a type of KWW1 model closely related to the KWW0, does not directly involve stretched-exponential temporal response [57], and is partly incorrect [35,56]. Nevertheless, the authors of the MFA deserve much credit for applying ideas from the mechanical relaxation area to electrical response

and developing a new and seminal approach to analyzing electrical dispersion data. In the past there has been considerable controversy over the usefulness for data fitting and interpretation of the MFA as compared to power-law model fitting (e.g. [5,9,54–56]). Thus it is particularly important to carry out a detailed evaluation of the utility of the two approaches, as is done here using the KWW1 model (the corrected MFA) and the ZC0.

Although the expression for KWW0 temporal response, included in Appendix A, is simple, there are no closed-form analytic expressions for KWW0 frequency response and for its associated DRT for arbitrary β. But with the inclusion in LEVM of means to calculate such quantities very accurately, it is has been possible for some time to use both KWW0 and KWW1 models for CNLS fitting of data with β a free parameter, as in the present work and in [35,49,56–58]. Note that although the empirical Davidson–Cole model [59], when defined as a CSD0 type, leads to response quite similar to that of the KWW0, CNLS fitting can readily discriminate between the two for ordinary data.

Since we shall be involved herein with using the KWW1 model to represent bulk CSD behavior, Fig. 2 shows the three types of peaked response to which this model leads, all normalized to a maximum value of unity and including a non-zero value of ϵ_{D_∞}. The limiting slopes shown are characteristic of those of such models as the KWW1 and Davidson–Cole CSD1 ones, those with intrinsic cutoff of their distributions of relaxation times at the high-τ end but none at the low-τ side [35,57,60]. Because all physically realizable models involve a smallest τ, $\tau_{\min}$, however, their DRTs must be cut off at this end as well, resulting in Debye-like high-frequency response at extremely high frequencies, ones beyond the usual immittance spectroscopy frequency range [43–46,57,60]. Then, as one approaches and reaches the cutoff frequency, $1/\tau_{\min}$, the high-frequency ϵ_s'' and M'' slopes of the figure change from $-\beta_1$ to -1 in the final limiting region. Here, where the data we consider does not extend to this region, no such small-τ cutoff is required, although it is an available option of KWW fitting using LEVM.

Incidentally, because of the extremely high resolving power of CNLS fitting, it is usually possible to discriminate adequately between response such as

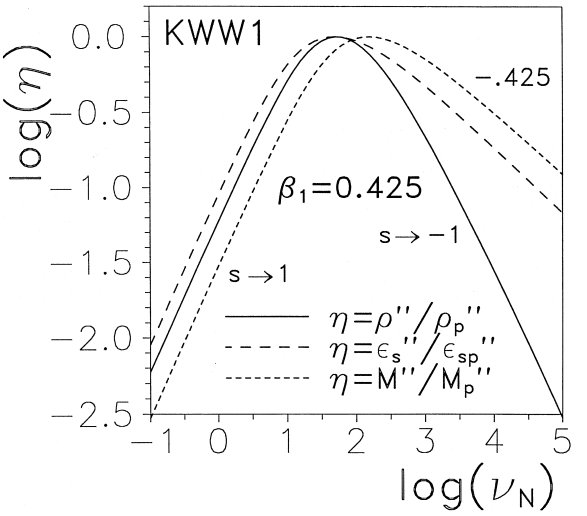

Fig. 2. Log–log curves comparing shapes of the three peaked, imaginary-part, frequency-response curves for the total KWW1 response model without cutoff, calculated using the KWW1-fit parameters for $Na_2O{\cdot}3SiO_2$ glass at $T=321$ K listed in Table 4 of [56]. These results are thus exact. All curves are normalized to unity at their peaks. Limiting log–log slopes, *s*, are shown. Here $\epsilon_s'' \equiv \epsilon'' - (\sigma_0/\epsilon_V\omega)$, thus removing the effect of σ_0 from the effective dielectric-loss curve. All curves shown here arise from conductive-system dispersion alone, but their peak values and shapes (but not limiting slopes) are affected by the value of ϵ_{D_∞}, present, here 4.8. The normalized frequency is defined as $\nu_N \equiv \nu/\nu_n$, where $\nu_n = 1$ Hz.

that of the KWW1 response model whose high-frequency limiting response is of power-law character in the absence of cutoff, and other models, such as that involving an exponential DAE, which lead to logarithmic response that approximates PLR quite closely over a limited but often considerable frequency range [61–63]. Such discrimination is only compromised for data with large errors and/or for data involving only a narrow frequency range.

2. Data fitting

2.1. Bulk- and electrode-model choice considerations

One possible reason for fitting a set of data is to discover a function that will fit the data very closely and so may be used to represent the data in con-

densed fashion and to allow interpolation and possibly even some extrapolation. But a more important reason is to find a well-fitting model whose structure and parameter values lead to increased understanding of the physicochemical processes occurring in the material. Sometimes one is more interested in electrode effects as opposed to bulk ones, or vice versa. But no matter which type of response, or both, is the area of primary interest one must ensure that the effects of all processes affecting the measured data are well represented in the complete fitting model. For high-resistivity CSD materials, such as disordered substances and wide-bandgap crystals, one is generally most concerned with bulk effects, and any electrode contributions are usually ignored, or are only mentioned briefly, but are rarely included in the full fitting model. Since, however, such contributions seem to be much more endemic than usually recognized for such materials, it is important that they be identified and well characterized in order to develop meaningful insights into bulk behavior.

Unless electrode effects are known to be unimportant or absent, as in some microwave measurements, one should allow the data themselves to answer the question of their importance. An early qualitative discussion of such effects appears in [17]. In the usual absence of a complete theoretical response model available for fitting, one will need to use an equivalent circuit for fitting, such as that of Fig. 1. The serious problem then arises of which individual fitting models one should use to represent the electrode effects and which for the bulk effects. Thus instead of the usual one-dimensional approach of trying just a PLR model, such as that of Eq. (5), one must search a two-dimensional choice space by carrying out fitting with different combinations of circuits to represent bulk behavior (assumed here to show either CSD or DSD but not both) and electrode effects.

Before any fitting is carried out, it is desirable to examine the frequency response of the data at all four of the immittance levels since they emphasize different aspects of the response. This can be readily done using LEVM. Then, one must choose at which immittance level to carry out the fit, what kind of weighting to use in CNLS fitting, and whether to fit the data with a CSD or DSD dispersion model (in the DEC or DED block of the Fig. 1 circuit).

2.2. Fitting criteria

A first fitting criterion should be that the combination model leads to a very good fit of the full data (real and imaginary parts simultaneously), one appreciably superior to that of the bulk model alone when electrode effects are non-negligible. Thus, CNLS fitting should be used when the data are available. This criterion is necessary but not sufficient. One can keep on adding parameters to the individual fitting circuits until a fit limited only by random errors in the data is achieved. But simplicity should be a goal as well, so the individual circuits should involve the minimum number of free parameters that allows the first criterion to be well satisfied. But even so, additional criteria are needed. Once one has obtained a likely composite fit, a program such as LEVM allows one to subtract the effects of the electrode circuit from the data, hopefully leaving only bulk effects, or vice versa. Both the individual circuits and the subtracted data must be examined for physical plausibility. For example, if either type of subtraction led to many negative real-part data points, the combination would be worthless for meaningful representation of a passive system.

Finally, a very important test should be carried out if the goal is best representation and understanding of bulk behavior. This test involves the comparison of the bulk-fitting parameter estimates and their estimated relative standard deviations, as obtained from the fit of the full original data with both electrode and bulk fitting models included, with those obtained from a fit to the electrode-subtracted data using only the same bulk response model as before. A good choice of the electrode and bulk models is then one in which the parameter estimates are closely the same and the relative standard deviations for the subtracted fit are comparable or smaller than the full-fit ones. Another important measure of the adequacy of a fit is the quantity S_F, which is the standard deviation of the relative residuals of the fit.

Next, if fits are carried out for a range of temperatures, it is necessary that the temperature dependencies of the estimated electrode- and bulk-model parameter values show plausible behavior. Whenever possible, it is also very desirable that measurements be made with different electrode separations in order

to allow unambiguous identification of bulk and electrode effects. The electrode parameters should be intensive, independent of electrode spacing, and before reduction to specific form some of the bulk ones, such as resistances, should be extensive. Finally, although it is often believed that electrode effects for a conducting situation contribute principally only to the low-frequency part of the response, this need not be so and, depending on measurement temperature, the reverse may be true, as we shall see.

2.3. Fitting results for $Na_2O{\cdot}3SiO_2$ glass data

2.3.1. Numerical results and discussion

In order to compare power-law fitting of a set of real data with other possible models one should, as discussed above, assess the importance of electrode effects by fitting with a composite model, and, if the parameters estimates of the best electrode-circuit model found are statistically significant, then subtract the electrode effects from the data before final model-comparison fitting of the subtracted data. Here, I shall illustrate the procedure by using the $T=321$ K data of Nowick and Lim for $Na_2O{\cdot}3SiO_2$ glass [5]. This data set and others covering a range of temperatures were previously fitted in [5] by Nowick and Lim and by me [49,56]. My fitting indicated some temperature-dependence irregularity of KWW1 β_1 estimates and disagreed strongly with those of the original analysis [5]. Incidentally, temperature-independent PLR estimates of the n of Eq. (5) herein led to 0.60 for the data of [5] and to 0.62 for later data and analysis of the same material [9] by Nowick and co-workers.

My earlier analyses of the 321 K data [49,56] followed the above composite-model procedure, investigated several combinations of bulk and electrode models, and suggested that a combination of a KWW1 model for bulk behavior and an electrode circuit consisting of a constant-phase element in parallel with an ideal capacitor provided a good fit of the data and led to a S_F value of about 0.0027. Subsequent work has shown that appreciably better results are obtained with the same KWW1 model and an electrode circuit made up of a ZC0 (parameters ρ_e, τ_e, and n_e) and an ideal capacitor, ϵ_e, in parallel with it. The estimates of these quantities using specific data were, respectively, about 1.4×10^7 Ω-cm, 4×10^4 s, 0.745, and 64. Ideally, if one is interested in the electrode parameters themselves, one should carry out the combined fit before converting the data from their original measured form, say at the impedance level, to their specific values at the complex resistivity level using a conversion factor involving electrode area and separation, but for simplicity this has not been done here.

Table 1 shows in the KWW1E line the parameter estimates of the KWW1 part of the full combined fit of the original data set. This fit, with proportional weighting [27,38], yielded a value of S_F nearly a factor of two smaller than that of the earlier analysis [56]. Although an appreciably smaller value than that in the table was found when a Havriliak–Negami model (a melding of the Davidson–Cole and ZC0 models) was used in place of the electrode-circuit ZC0, subtraction led to negative σ' values above a mid-frequency point, strongly precluding the use of this model. All fit results shown in this table and in the succeeding one were carried out at the complex-conductivity immittance level. For simplicity, a composite fitting model involving CSD and DSD dispersion in parallel (see [42]), as in Fig. 1, has not been investigated here but is worthy of future investigation with and without a series electrode contribution.

Table 1
LEVM CNLS fitting results for $Na_2O{\cdot}3SiO_2$ glass data at 321 K[a]

Model	Data	$100S_F$	$1000\tau_o$	ψ	$10^{10}\sigma_0$	ϵ_∞
ZC0	Full-A	2.38	1.42	0.645	6.428	9.41
KWW1E	Full-B	0.141	0.117	0.623	6.914	6.86
KWW1	NE	0.138	0.118	0.623	6.914	6.84
KWW0	NE	1.54	1.33	0.552	6.951	10.55
KWW0P	NE	0.462	2.51	0.575	6.912	10.51
ZC0	NE	2.91	1.36	0.607	6.364	10.44

[a] Complex conductivity fitting using proportional weighting. Full data situation: (A) ZC0 model alone; (B) KWW1E denotes a KWW1 model and electrode-fit parameters (see text). NE, effects of electrode parameters removed from data using KWW1E fit. The quantity ψ is n for the ZC0, $(1-\beta_1)$ for the KWW1, and β_0 for the KWW0 model, and the dielectric quantity ϵ_∞ is discussed in Section 2.3.1. KWW0P indicates that the model includes a conductivity element, σ_p in parallel with ϵ_∞ (represented by the C_∞ of Fig. 1). Here its estimated value was about 2.456×10^{-10} mho/cm, and this value was used in calculating the σ_0 value shown in the table for the KWW0P line. When units are not explicitly mentioned, they are mho/cm for σ quantities and seconds for τ ones.

It is worth mentioning that the use of the usual CSD0 Davidson–Cole model for the electrode circuit led to slightly worse results than those for the KWW1E model listed in Table 1, but a KWW0 electrode-circuit model yielded ones virtually identical to the KWW1E ones. Evidently, the nonphysical behavior of the electrode-circuit ZC0 at the low-frequency end of the data has little effect on the fit since in this region, as we shall see later, electrode effects are much smaller than bulk ones for the present data.

The line marked Full-A in Table 1 shows the results of a ZC0 fit of the original data without an electrode circuit and is very much poorer than the corresponding KWW1E fit which does. Note that CSD1 fits, such as that using the KWW1, lead to an ϵ_x estimate of the true dipolar dielectric constant, ϵ_{D_∞}, while CSD0 ones, such as the KWW0 and ZC0 ones in the table, provide estimates of $\epsilon_x = \epsilon_\infty \equiv \epsilon_{D_\infty} + \epsilon_{C_\infty}$, where ϵ_{C_∞} (actually the CSD1 quantity $(\epsilon_{C_\infty})_1$ defined in Appendix A is a high-frequency-limiting effective dielectric constant arising solely from mobile charges (see Appendix A for its calculation and for other details) [35,36,56]. Here its value, calculated from other parameter estimates using Eq. (A.10), was about 3.61.

The reason why the free fitting parameter ϵ_x is different for CSD0 and CSD1 situations is that $(\epsilon_{C_\infty})_1$ is non-zero for non-cutoff CSD1 response when ρ_∞ is zero, but $(\epsilon_{C_\infty})_0$ is zero for usual non-cutoff situations. Thus, because a CSD1 model implicitly includes the mobile-charge high-frequency-limiting dielectric constant contributions present in the data, ϵ_x need not do so and is free to estimate ϵ_{D_∞} directly. But for CSD0-model fits of experimental data ϵ_x must take account of both the ϵ_{C_∞} and ϵ_{D_∞} effects present in the data.

Although no ZC0E fit results are shown in Table 1, it was found that using two ZC0 models in series yielded the best result: an $S_F \simeq 0.0037$ for both electrode and bulk effects together. No ϵ_e could be estimated but an ϵ_x value of 12.2 was found, along with a bulk $n \simeq 0.59$ value and an electrode $n_e \simeq 0.96$ value, almost Debye behavior. When the electrode effects were subtracted from the data and a ZC0 fit carried out, the electrode-fit criterion discussed above was not satisfied: the S_F value was 40% larger, the parameters were somewhat different from the corresponding ones estimated by the combined fit, and the σ_0 estimate was far from those shown in Table 1. Thus, it is quite clear that a bulk KWW1 model is far superior to a ZC0 one for fitting the original data.

It is a common misconception that adding additional free parameters to a fit, while it may improve the fit itself, generally leads to less accurate estimates of the original parameters. Although its results are not explicitly included in Table 1, a four-parameter CNLS KWW1 fit of the full data without an added electrode circuit led to a fit with an S_F value more than 25 times larger than that for the KWW1E fit included in the table. When the fit included the four additional electrode-circuit free parameters as well (i.e., the KWW1E fit), the estimated standard deviations of the four free bulk parameters decreased by factors of from 3.5 to 10.8, showing that when several appropriate free parameters are added to a fit model, the estimated uncertainties in the original parameters may be significantly reduced.

Although Table 1 includes no parameter relative standard deviation estimates, it is natural to wonder what happens to those for the bulk parameters when a fit such as that designated KWW1 in Table 1, which involves data with estimated electrode effects subtracted, is carried out. Even though there is only a negligible difference between the S_F values and bulk-parameter estimates of the KWW1E and KWW1 fits shown in the table, the relative standard deviations of the four bulk parameters were found to decrease by factors of about 3 to 9 for the KWW1 fit as compared to those for the KWW1E one. These fitting results suggest that not only is it worthwhile to fit good data with electrode parameters as well as bulk ones, but it may be then desirable to use such fit results to eliminate any significant electrode effects from the data and then fit the modified data to obtain final bulk parameter estimates and uncertainties.

All NE results in the table and in the subsequent graphs involve data obtained from the KWW1E fit followed by subtraction of the electrode-circuit effects. Do the KWW1 NE parameter estimates satisfy the criteria and test described above? They do so almost perfectly, with the slight difference between the KWW1E and KWW1 NE ϵ_x estimates arising from roundoff alone. Another test, one quite closely satisfied by the KWW1E model, is to compare the fit

of this combined model at the complex resistivity level with that shown in the table for the complex conductivity level. Such fits should yield closely similar results if systematic errors in the fitting are negligible.

The above results suggest that it is plausible to identify the present subtracted data set as a close approximation of the data that would have been found if they had been measured without electrode effects. We see that both before and after subtraction the ZC0 fits are very much poorer than the KWW1 ones and their parameter estimates are mostly correspondingly less accurate. Incidentally, fits of the NE data were also carried out with the ZC1 model and led to a large S_F value of about 0.28 without taking account of electrode effects and of about 0.11 when the most appropriate electrode circuit was used as well, both completely unsatisfactory fittings.

The present use of the KWW1 model in the composite fitting circuit does not necessarily imply that this is the best model to fit the subtracted data. Nevertheless, NE results for the several choices included in the table and others indicate that the KWW1 is indeed the preferred model of those investigated. Not shown are results for even poorer fittings with an exponential DAE and with several other models. Although we see that the KWW0 model yields an appreciably better fit than does the ZC0 one, the fit is still relatively poor and the parameter estimates are also dubious. It has been shown that for KWW0-model fits of conductive- or dielectric-system data the addition of a conductance in parallel with the C_∞ element of Fig. 1 can often lead to appreciably smaller S_F values, although the added element may sometimes need to be negative [58] and should not be taken as physically significant. The model designated KWW0P in Table 1 is of this type, and although the fit and most of the parameter estimates are improved, it is still far less appropriate than that obtained with the KWW1 model.

Although the CSD1 and CSD0 estimates of τ_0 shown in Table 1 are quite different, the corresponding estimates of $\langle\tau\rangle$ are much closer. The high-frequency-limiting σ' slopes of the KWW1, KWW0, and ZC0 models are [49] $(1-\beta_1)$, β_0, and n, respectively, and are shown in column ψ of the table. For fitting of the same data set, one might expect that all the ψ values shown in the table would be good estimates of the actual limiting slope. The differences in the NE values listed arise primarily, however, from intrinsic differences in the models themselves. For example, if the NE data set is replaced by data calculated exactly from the KWW1 NE model and parameter estimates, one finds that fitting with ZC0 still yields $n \simeq 0.607$. On the other hand, KWW1 fitting of exact data, extending to $\nu = 10^5$ Hz and calculated with the the ZC0 NE model and parameters, led to $(1-\beta_1) \simeq 0.72$ and only closely approached 0.623 when the range extended to 10^9 Hz, a type of windowing effect [6,12,42]. It is also clear from the present results that the relation $\beta_0 + \beta_1 = 1$ [49,58] only holds approximately here, although other KWW0 fits of accurate KWW1 data show close satisfaction of this relation when a free σ_p parameter is included in the fit [58].

Although the ψ values shown in Table 1 are all comparable, it is interesting that when β_1 is large, say 0.8, and the KWW1 response then approaches Debye type, KWW0 fitting of such simulated KWW1 data still leads closely to the expected value of $\beta_0 = 0.20$, but ZC0 fitting of the data is poor and its estimates are discrepant. For example, full CNLS fitting yields an n estimate of about 0.52, but n estimates for real- and imaginary-part fitting are about 0.34 and 0.93, respectively, with the S_F values being smallest for imaginary-part fitting and largest for the CNLS fit. Such large differences are an immediate indication that the ZC0 is not appropriate for fitting KWW1-type data when it approaches Debye response. In addition, parameter estimates from such ZC0 fits depend appreciably on the width and placement of the data frequency-window, unlike those included in the present tables.

For the present full data, $\epsilon'(\omega)$ approaches a plateau value as ω decreases: namely, the low frequency-limiting effective dielectric constant, $\epsilon_{C_0} + \epsilon_{D_\infty}$, about 30 for the KWW1E fit. Since closely the same value was found for the KWW1 NE fit, it seems clear that electrode effects do not influence this value for the present 321 K trisilicate data. The increase in $\epsilon'(\omega)$ towards a low-frequency plateau for the present data is exceptionally well described by the model prediction for $\epsilon_C(\omega)$ and so is highly unlikely to involve either a dipolar dielectric dispersion effect or an electrode one.

A progressive rise of $\epsilon'(\omega)$ at low frequencies for trisilicate data like that considered here, as well as for other materials, increases in magnitude as the temperature increases and has been ascribed to blocking at the electrodes [5,9,11]. This explanation may be rejected for the present data fits, but it is possible that some part of the increase at higher temperatures may indeed be associated with electrode effects. As shown by the present results, the matter may be resolved by the present fitting/analysis methods.

Because most earlier fits using the ZC0 or an equivalent model have been carried out using only real-part conductivity data, and, when least-squares fitting is used at all, unity weighting is usually employed, possibly with different fits for different data ranges [9], it is of interest to compare KWW1 and ZC0 fit results for σ' data with proportional or unity weighting. In addition, for comparison I have included imaginary-part fits as well. Such results are presented in Table 2. For a well-fitting appropriate model, one would expect that the parameter estimates obtained under the above conditions should be quite close to those obtained with full CNLS fitting. We see that this is indeed the case for the various KWW1 fits, but is far from the case for most of the ZC0 estimates. Although no estimate of ϵ_x can be obtained with real-part-only fitting at the complex conductivity level, and no σ_0 estimates are possible with imaginary-part ZC0 fitting, such σ_0 estimates are obtainable for both imaginary- and real-part KWW1 fitting. Note particularly the poor estimates obtained with ZC0 fitting for both n and σ_0, matters that are further discussed below.

Table 2
LEVM NLS fitting results for $Na_2O{\cdot}3SiO_2$ glass data at 321 K[a]

Model	Data, Wt	$100S_F$	ψ	$10^{10}\sigma_0$	ϵ_x
KWW1	R, P	0.122	0.622	6.912	–
KWW1	I, P	0.150	0.625	6.861	6.91
ZC0	R, P	0.860	0.584	5.979	–
ZC0	I, P	2.10	0.671	–	9.86
KWW1	R, U	0.232	0.624	6.940	–
KWW1	I, U	0.590	0.615	7.102	6.74
ZC0	R, U	1.33	0.588	6.169	–
ZC0	I, U	5.94	0.580	–	10.52

[a] Real-part (R) or imaginary-part (I) fitting of $\sigma(\omega)$ data with electrode effects removed. Proportional weighting (P) or unity weighting (U). See the caption of Table 1 for symbol identifications.

The present fitting results show unequivocally for the present data that KWW1 fitting is much superior to ZC0 PLR fitting whether one deals with real, imaginary, or full complex data, in agreement with earlier results for different materials and temperatures [35,36,49,56]. But the literature suggests differently. As an example, see [8,55] where detailed comparison of power-law and KWW1/modulus formalism [52,53] fitting approaches is carried out for an ion-conducting glass. A conclusion of this work was that power-law fitting led to fits superior to those obtained with the modulus formalism approach [8]. A general perception of past modulus-formalism fitting is that it "... commonly cannot fit the high-frequency wing of M''" (in [8], see also [5,55]). This problem even appeared in the first modulus-formalism work [53]. Here, no such discrepancy is present, and the KWW1-fit $|M_1''|$ relative residuals are of the order of 0.001 over the whole frequency range. The difference arises because the present work involves accurate CNLS fitting and does not neglect ϵ_{D_∞} and electrode effects, as do usual MFA fits.

2.3.2. Some graphical comparisons

Although detailed CNLS fitting results, as shown in Tables 1 and 2, are necessary for deciding on an appropriate model to describe the data and for estimating model parameter values accurately, graphical comparisons of the data and fit results are also important and can often elucidate behavior not obvious from fit numbers alone. Thus, Fig. 3 shows, on comparing the KWW1E fit of the original σ' data to the KWW1 fit curve of the data with electrode effects subtracted (KWW1, NE), that here electrode effects are only significant toward the high-frequency end of the response. It is also clear that the ZC0 fit of the subtracted data appears good on a log–log plot except at the lowest frequencies. The low-frequency difference is better illustrated by the two $\Delta\sigma$ curves included in the graph. The slope of the KWW1 one approaches its physically realizable proper value of 2 as the frequency decreases but that of the ZC0 curve approaches its nonphysical limiting value of n, here about 0.61, as shown in Table 1. It is this difference that can lead to inadequate ZC0 estimates of σ (such as those in the tables) unless the experimental data

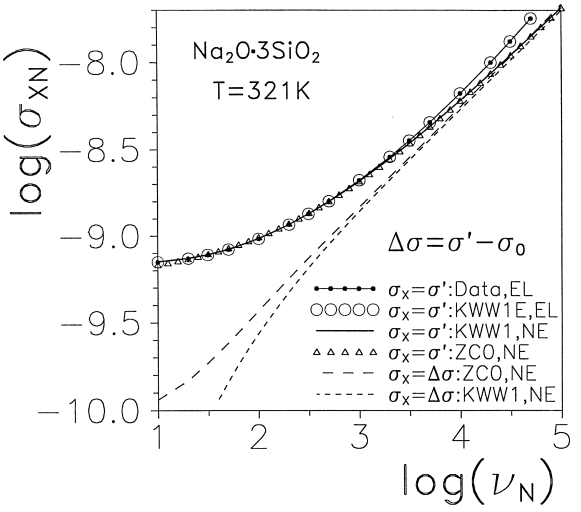

Fig. 3. Complex nonlinear least squares (CNLS) fit results for σ' obtained with different fitting models. Here 'EL' denotes that the full original data were used without subtraction of electrode effects; 'NE' indicates that such subtraction has been made using the LEVM computer program; $\sigma_{XN} \equiv \sigma_X/\sigma_n$, where $\sigma_n = 1$ Ω-cm; and $\Delta\sigma \equiv \sigma' - \sigma_0$. See the caption of Table 1 for more details and definitions. The KWW1E fit of the full data involved electrode circuit parameters as well as those of the KWW1 bulk model. The effects of these electrode parameters, whose values were estimated in the KWW1E fit, were subtracted from the original data to yield the 'NE' modified data. The resulting data set was then fitted to obtain the new dispersion-model 'NE' parameter estimates shown in Table 1. Finally, these estimates were used to generate synthetic data with many more points than were present in the original data set and to extrapolate the response when required. Thus, the 'NE' curves shown here are high-resolution consequences of the original 17-point modified data fits.

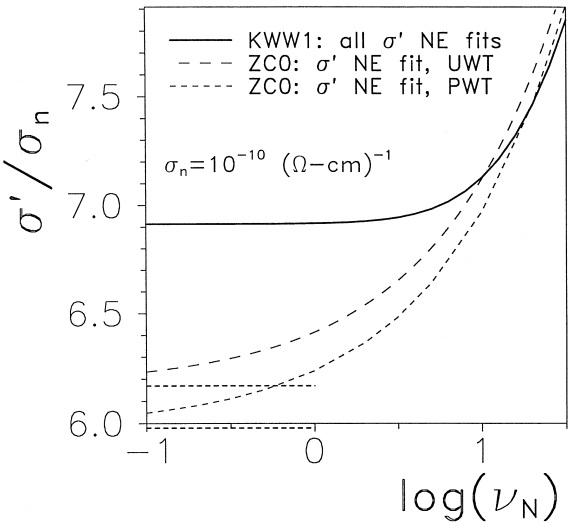

Fig. 4. Extrapolated low-frequency response of real-part fitting results for σ' NE-data with two dispersion models. The horizontal short-dashed lines show the limiting low-frequency estimates of σ_0 for the ZC0 model (Eqs. (6) or (7)) with proportional weighting (PWT) and with unity weighting (UWT). Note that σ_n is 10^{-10} mho/cm here, not the 1 mho/cm used otherwise.

extend far enough into the low-frequency-limiting constant-σ' region itself. In the interest of simplicity, the ZC0 fit of the full data (designated Full-A in Table 1) is not shown in Fig. 3, but the real- and imaginary-part relative residuals for this rather poor fit are about 10 times larger than those for the good KWW1E fit of the same data (designated Full-B).

Problems arising from the use of ZC0 real-part fitting of the subtracted data to try to obtain a good estimate of σ_0 are illustrated in Fig. 4 by the linear plot of fit predictions for frequencies extrapolated to 0.01 of the lowest measured frequency. The horizontal short-dash lines show the asymptotic ZC0 σ_0 predictions, ones still not reached even at the frequency of 0.1 Hz. A word (or figure) to the wise should be sufficient.

Because bulk and electrode effects are in series electrically, their separate effects are best illustrated by plots at the complex resistivity level, as in Fig. 5. Shown in this figure are extrapolated curves calculated from the KWW1E fit parameters without and with subtractions. They indicate that here electrode effects are more than 100 times smaller than the bulk ones at low frequencies, that the imaginary parts are somewhat less than 10 times smaller at high frequencies, and that the real parts become comparable as the frequency increases. Note that the limiting high-frequency slopes of the KWW1 response are -1 for the imaginary part and $-(1+\beta_1)$, here about -1.38, for the real part. These slopes and those of the electrode-only ZC0 are in agreement with the table of limiting slopes presented in [49].

The dependencies of the various σ' slopes on frequency are also of interest and are shown in Fig. 6. At high-frequencies the KWW1 and ZC0 bulk slopes approach the ψ values listed in Table 1, and that for the electrode-only ZC0 response approaches its $n_e = 0.745$ value. Notice particularly the differences between the full-data KWW1E and ZC0 slopes. The slope of the data and its KWW1E

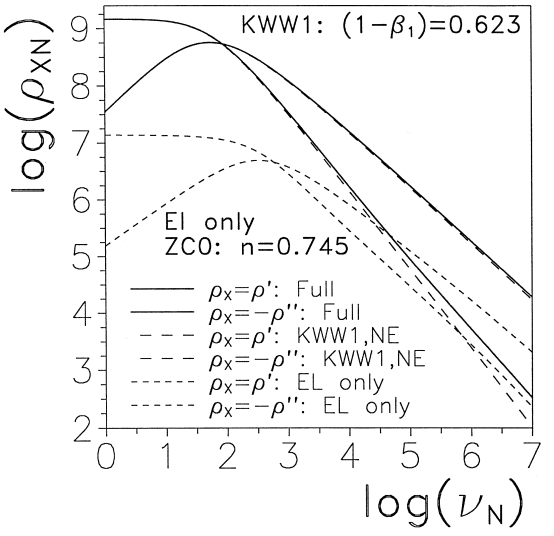

Fig. 5. Log–log plots at the complex resistivity level of extended response derived from the CNLS fit of the original data using the composite KWW1E model. Here $\rho_{xN} \equiv \rho_x/\rho_n$, where $\rho_n = 1$ Ω-cm. Real and imaginary responses are shown for the full data, for the no-electrode KWW1-contribution part, and for the separate electrode contribution, designated 'El only' and involving a ZC0 model in parallel with an ideal capacitance (see Fig. 1 and the text).

extrapolation continues to increase up to much higher frequencies than does that of the ZC0-alone fit of the same data. This continuous increase of the slope up to 0.8 or so, arising here from the presence of electrode effects, may possibly explain why considerable data leading to the master plot of Roling [64] exhibits similar continually increasing slope that does not reach unity in the frequency range shown [65].

If one calculates the slope of $\Delta\sigma \equiv (\sigma'(\omega) - \sigma_0)$ for the ZC0 model of Eq. (6) one would expect to obtain the frequency-independent value of n. An alternative method of checking data for constant n is to use Eqs. (A.16) and (A.18) of Appendix A to calculate the test parameter $n_t = n_{tk}$. We have made such calculations for some of the situations included in Table 1 and show the results in Fig. 7. These calculations used the estimates shown in the table for the subtracted-fit quantities ϵ_x and σ_0. We see that the use of these best estimates of the ZC0 subtraction quantities led to appreciable and systematic n_t variation with frequency when the raw data were used, with and without subtraction of electrode effects. When the same estimates were applied to the fit-prediction calculated data sets, the virtually constant estimates of n_t shown in the figure, and equal to the

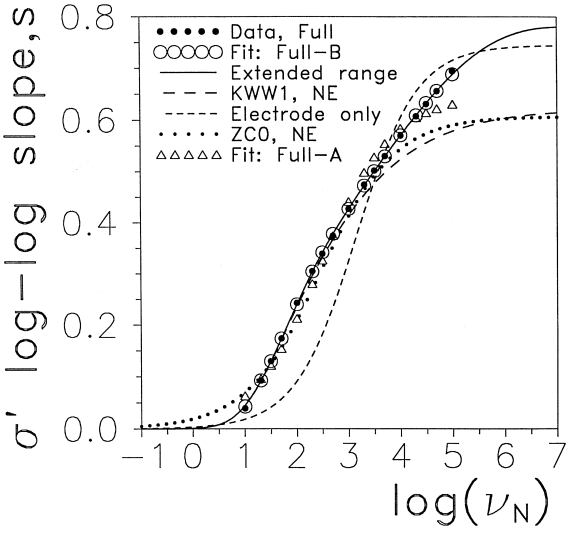

Fig. 6. Log–log slopes versus log frequency for the original full data, the CNLS fit of the composite KWW1E model, that fit extended, the ZC0 fit of the full data, KWW1 and ZC0 fits of the NE-data, and the electrode-only part of the full data.

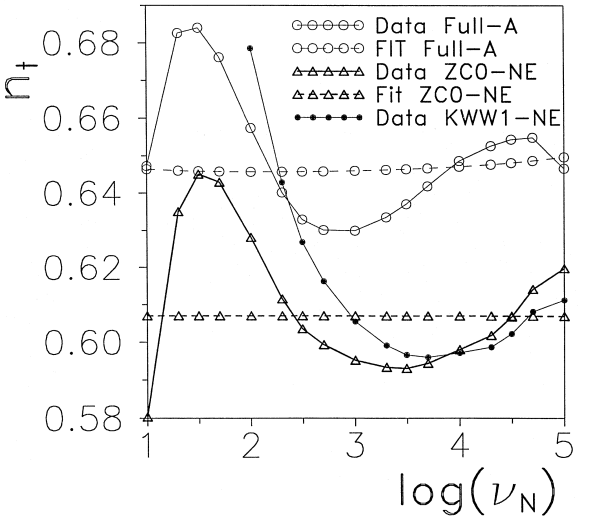

Fig. 7. Plots of the n_{tk} test quantity of Eq. (A.18) versus frequency for some of the data and fit situations of Table 1, with $k = 0$ for the top four lines listed and $k = 1$ for the bottom KWW1-NE one.

n values listed in the table, were obtained. The slight upward curvature at high frequencies of the n_{t0} line obtained using the ZC0 Full-A fit values evidently arises from electrode effects since it disappears when they are removed.

The systematic deviations from a constant n_{t0} value for the ZC0 data curves indicate that the ZC0 is not a particularly appropriate choice for fitting the present data, as already indicated by the S_F values in Table 1. It was found that the n_{t1} values for both the original data and for the KWW1 fits yielded variable values quite close to unity over the full range when the proper $\epsilon_x = \epsilon_{D_\infty}$ estimates were used in the subtraction of Eq. (A.16). When the fit prediction value of ϵ_∞ was used instead, both the original data and the subtracted data led to very closely the same results, that shown for the KWW1-NE curve of the figure. As the curve shows, even the use of such an incorrect value cannot yield frequency-independent values of n_{t1}. So clearly this test indicates, as one expects, that the data are again not of pure PLR form.

Curves of the R_0 of Eq. (A.17) calculated from the data for an ion-conducting glass appear in [8] and in [55] but are less instructive than had they presented n_t directly. They show a substantially constant value of R_0 over several decades followed by a large rise toward the low-frequency end of the data. These increases may be associated with the non-physical character of the PLR law at low frequencies and/or with an inadequate choice of the subtracted σ_0 value.

3. Summary

The KWW1 model for bulk dispersion has proved appreciably superior to others for fitting much dispersed bulk data for conductive systems. But for the experimental data investigated herein it was found that the inclusion of an electrode response model as well as a KWW1 bulk response model led to a much improved and very precise fit. In addition, it has been demonstrated that a free effective dielectric parameter, ϵ_x, should always be included in any composite model used for fitting conductive system data. This parameter estimates the high-frequency-limiting dipolar dielectric constant, ϵ_{D_∞}, for CSD1 bulk models such as the KWW1. On the other hand, for CSD0 models such as the KWW0 and the ZC0, ϵ_x provides an estimate of the full high-frequency-limiting effective dielectric constant, $\epsilon_\infty = \epsilon_{C_\infty} + \epsilon_{D_\infty}$, a quantity that includes contributions from both mobile monopolar and non-mobile dipolar charge.

The original, uncorrected electric modulus formalism, still widely used for conductive-system data analysis, incorrectly involves ϵ_∞ instead of ϵ_{C_∞}, and it has nearly always been applied without taking proper account of the influence of ϵ_{D_∞}. Useful criteria for choosing appropriate bulk and electrode fitting models have been discussed and illustrated. The present results indicate that power-law UDR models are not universal and should probably be used only for preliminary fitting. Finally, possible high-frequency effects associated with electrode contributions to the total response, as illustrated herein, may explain some or all of the tendency for the slope of $\sigma'(\omega)$ to increase at high frequencies, as observed for many materials [64,65].

Definitions of acronyms and of principal symbols

CNLS	Complex nonlinear least-squares
CSD	Conductive-system dispersion
CSDk	Two types of CSD response with $k=0$ or 1; see Eq. (A.1)
DAE	Distribution of activation energies, E
DRT	Distribution of relaxation times, τ
DSD	Dielectric-system dispersion
KWW	Kohlrausch–Williams–Watts response model
KWWk	KWW response defined by index k, where $k=0$ or 1; see Appendix A
KWW1E	Composite response model using KWW1 for bulk response and ZC0 for electrode response
LEVM	The complex-nonlinear-least-squares fitting program used herein
MFA	Electric modulus formalism approach
NE	Designates data from which electrode effects have been removed
PLR	Power law response model
PWT	Proportional weighting in CNLS fitting
UDR	Universal dynamic (or dielectric) response

UWT	Unity weighting
ZC	A specific power-law response model; see Eq. (6) for the ZC0 form
ZCk	ZC response defined by index k, where $k = 0$ or 1
x, y	$x = \tau/\tau_o$; $y = \ln(x)$
$\langle x^m \rangle_k$	Dimensionless mth moment of a distribution; see Eq. (A.4)
$F_k(y)$	A normalized DRT involving the logarithmic variable y. Equal to $xG_k(x)$
$G_k(x)$	A normalized DRT associated with $I_k(\Omega)$. See Eq. (A.1)
$I_k(\Omega)$	Normalized dispersion response function; it does not include any effects of a non-zero ρ_∞ or of ϵ_{D_∞}. See Eqs. (A.1)–(A.3)
$M(\omega)$	Also denoted as $M_{Tk}(\omega)$. Complex modulus response calculated from data that (necessarily) includes ϵ_{D_∞} effects or from a model that does so
$M_1(\omega)$	Complex modulus function for pure CSD1 model response, such as KWW1, or for data with ϵ_{D_∞} effects removed
n	Exponent in PLR response such as the ZC0 model
S_F	Relative standard deviation of a fit. It is the standard deviation of the relative residuals or, equivalently, the relative standard deviation of the residuals themselves
β	$\beta = \beta_0$, the exponent in stretched-exponential KWW0 temporal response
β_k	KWWk shape parameter for $k = 0$ or 1
β_{01}	The value of β_0 used in the MFA calculation of KWW1 response; $\beta_{01} = \beta_1$
$\epsilon(\omega)$	Full complex dielectric response function. In the absence of true dielectric-system dispersion in the frequency range of interest, $\epsilon(\omega) = \epsilon_C(\omega) + \epsilon_{D_\infty}$
$\epsilon_C(\omega)$	CSD effective dielectric response arising solely from mobile charges; $k = 0$ or 1
ϵ_{C_0}	Abbreviation for $\epsilon_C(0)$
ϵ_{C_∞}	Abbreviation for $\epsilon_C(\infty)$
ϵ_{D_∞}	High-frequency-limiting true dielectric constant arising from dipolar effects
$\epsilon_s(\omega)$	Reduced complex dielectric constant: $\epsilon(\omega) - i(\sigma_0/\epsilon_V\omega)$
ϵ_∞	Abbreviation for $\epsilon(\infty) \equiv \epsilon_{C_\infty} + \epsilon_{D_\infty}$
ϵ_V	Permittivity of vacuum
ν_N	Normalized frequency, ν/ν_n, with $\nu_n = 1$ Hz
$\rho(\omega)$	Resistivity for $k = 0$ or 1, a complex quantity
ρ_0	Abbreviation for $\rho(0)$
$\sigma(\omega)$	Conductivity for $k = 0$ or 1; $\sigma(\omega) = \sigma'(\omega) + i\sigma''(\omega)$
τ_{min}	The minimum relaxation time for a response model such as a DRT with cutoff
τ_o	Characteristic relaxation time of a response model
$\Phi(t)$	Macroscopic temporal relaxation function

Appendix A. Summary of some CSD, DSD, and MFA relations

It is useful to define three kinds of dispersive response, ones distinguished here by the index k [49,56]. Let $k = \mathrm{D}$ denote dielectric dispersion [DSD], and $k = 0$ and 1 denote two kinds of conductive-system dispersion, CSD0 and CSD1. Now define U_k as an unnormalized measured or model quantity of interest, such as an impedance or complex resistivity, or a complex dielectric constant. It is mathematically convenient to express the normalized form of U_k, namely I_k, in terms of a DRT, say $g_k(\tau)$. This is always possible for any reasonable response model and does not necessarily imply that a physically significant DRT is present. Here U_k involves only a single dispersion process and does not include electrode effects.

Let $x \equiv \tau/\tau_{ok}$, where τ_{ok} is a characteristic response time of the fitting model and define $y \equiv \ln(x)$ and $G_k(x) = \tau_{ok} g_k(\tau)$. We may now define the normalized response quantity $I_k(\omega)$ as

$$I_k(\omega) \equiv \frac{U_k(\omega) - U_k(\infty)}{U_k(0) - U_k(\infty)} = \int_0^\infty \frac{G_k(x)\,\mathrm{d}x}{[1 + i\omega\tau_{ok}x]} = \int_{-\infty}^{\infty} \frac{F_k(y)\,\mathrm{d}y}{[1 + i\omega\tau_{ok}\exp(y)]}, \quad \text{(A.1)}$$

where

$$U_k(\omega) = U_k'(\omega) + i\delta_k U_k''(\omega), \quad \text{(A.2)}$$

and

$$I_k(\omega) = I'_k(\omega) + i\delta_k I''_k(\omega). \tag{A.3}$$

Here we follow the usual sign conventions and set the quantities δ_0 and δ_1 in Eqs. (A.2) and (A.3) equal to 1 and δ_D equal to -1. The F_k form of the distribution may be simply related to a distribution of activation energies for a thermally activated situation [47] and is given by $F_k(y) \equiv xG_k(x)$. Since the DRTs are taken normalized in the above, it follows that $I_k(0) = 1$ and $I_k(\infty) = 0$.

Finally, the dimensionless moments of a $G_k(x)$ distribution are defined as

$$\langle x^m \rangle_k \equiv \int_0^\infty x^m G_k(x)\, dx, \tag{A.4}$$

so when τ_o is the characteristic relaxation time of a DRT, the situation considered here, its average over the distribution is $\langle \tau \rangle_k = \tau_o \langle x \rangle_k$. I have usually suppressed use of the k subscript for such quantities as τ_o, x, y, ρ, and σ. Note that in the absence of dispersion, where we deal only with Debye relaxation response, which may be represented by a single resistor and capacitor connected together, we may take $G_k(x) = \delta(x - x_{ok})$ with $x_{ok} = 1$. It follows that the dimensionless moments of a Debye distribution are all unity.

It is important to emphasize that the choice $k = D$ specifies that the U_D response of Eq. (A.1) refers to only that part of the complex dielectric constant $\epsilon(\omega)$ (or corresponding complex capacitance) associated with dispersion and thus involves a distribution of dielectric-system relaxation times, directly related to the Maxwell circuit, one made up of M (a pure number here) combinations of a resistor and capacitor in series, all in parallel [27,61,66]. For pure DSD response, no σ_0 is present, and if it is found experimentally that σ_0 is non-zero, it will not be associated with dipolar effects and will thus be uncorrelated with $\Delta\epsilon_D \equiv \epsilon'_D(0) - \epsilon'_D(\infty)$, an overall dielectric-dispersion-strength quantity. Here $\epsilon'_D(\infty) \equiv \epsilon_{D_\infty}$.

On the other hand, the choices $k = 0$ and $k = 1$ specify CSD response at the complex resistivity $\rho(\omega)$ (or impedance) level and thus involve, through G_0 and G_1, distributions of conductive-system relaxation times that are directly related to the Voigt circuit, one involving M combinations of a resistor and capacitor in parallel, all in series [27,61,66]. Thus, it is evident that CSD and DSD distributions represent different physical processes, but it has been found that, with the inclusion of one or two additional fitting parameters, DSD response, including a non-zero σ_0, may be closely fitted by a CSD model and vice versa [58]. Let us define, for $k = 0$ or 1, $\Delta\rho_k \equiv \rho'_k(0) - \rho'_k(\infty)$, the strength of pure CSD, and take $\rho'_k(\infty) \equiv \rho_{k\infty}$, usually written as just ρ_∞. Also set $\rho'_k(0) \equiv \rho_{k0} = \rho_0 = 1/\sigma_0$. Note that for CSD σ_0 will always be non-zero and will be directly related to the ac response. Further, one must always take account of a non-zero ϵ_{D_∞} when fitting CSD response models to experimental data.

The $G_0(x)$ and $G_1(x)$ CSD distributions are closely related. When a specific form of G_0 is known, one that might even be formally identical to G_D, the associated normalized G_1 is, by definition [35,36,56], given by

$$G_1(x) = [x/\langle x \rangle_0] G_0(x), \tag{A.5}$$

where the value of any shape parameter appearing in $G_0(x)$ is that for $G_1(x)$. Thus for the KWW situation, for example, the β_0 parameter of the KWW0, which is the same for both the KWW0 frequency response and its stretched-exponential temporal response, is used for the KWW1 model. To distinguish the β_0 used for this purpose in calculating the KWW1 $G_1(x)$ from that present when the ordinary KWW0 model is directly used for fitting, designate the former as β_{01}, so $\beta_1 = \beta_{01}$. Fitting of the same data by the KWW0 and KWW1 models leads to estimates of the different quantities $\beta_0 (\neq \beta_{01})$ and β_1, respectively, with, ideally, $\beta_1 = 1 - \beta_0$. Eqs. (A.4) and (A.5) lead to

$$\langle x \rangle_0 = 1/\langle x^{-1} \rangle_1, \tag{A.6}$$

where $\langle x \rangle_0$ involves β_{01}.

The G_1 distribution involves both different frequency and temporal response than those of the $G_0(x)$. Thus, for example, although KWW0 temporal response is of stretched-exponential form, $\Phi(t) = \exp[-(t/\tau_o)^{\beta_0}]$, that associated with the KWW1 (or MFA) $G_1(x)$ distribution and its frequency response is not of such form [57], a matter usually misunderstood (or at least not made clear) in the past (e.g. [29]).

Now Eqs. (A.1), (A.5), and (A.6) lead to the following relation between $I_1(\omega)$ and $I_0(\omega)$ [56]:

$$I_1(\omega) = [\langle x^{-1}\rangle_1/(i\omega\tau_o)][1 - I_0(\omega)], \quad \text{(A.7)}$$

where $I_0(\omega)$ involves β_{01}. Note that if $I_0(\omega) = 1/[1 + i\omega\tau_o]$, simple Debye response, then $I_1(\omega) = I_0(\omega)$. The response at the complex modulus level associated with $I_1(\omega)$ is, from Eq. (A.1), $M_1(\omega) = i\omega\epsilon_V[\rho_\infty + \Delta\rho_1 I_1(\omega)]$, which leads, in the usual case of $\rho_\infty = 0$, to

$$M_1(\omega) = [\epsilon_V\rho_0\langle\tau^{-1}\rangle_1][1 - I_0(\omega)], \quad \text{(A.8)}$$

where we have used $\Delta\rho_1 = \rho_{10} \equiv \rho_0$. When this equation is employed for experimental data fitting, all parameters are those for CSD1 response, so a separate free parameter representing ϵ_{D_∞} must be included in the full fitting model [35,36,56,58].

Conductive-system dispersive response leads to non-dipolar dielectric effects of its own, here denoted by the complex quantity $(\epsilon_C(\omega))_k$ for $k = 0$ or 1 [56]. For example, one finds, for any I_0 or I_1 response model that can be expressed in terms of a DRT, the following high- and low-frequency limiting relations when $\rho_\infty = 0$ or its effects have been subtracted from the data [56,65]

$$(\epsilon_{C_\infty})_0 = (\sigma_0\tau_o/\epsilon_V)/\langle x^{-1}\rangle_0, \quad \text{(A.9)}$$

$$(\epsilon_{C_\infty})_1 = (\sigma_0\tau_o/\epsilon_V)/\langle x^{-1}\rangle_1 = (\sigma_0\tau_o/\epsilon_V)\langle x\rangle_0, \quad \text{(A.10)}$$

$$(\epsilon_{C_0})_0 = (\sigma_0\tau_o/\epsilon_V)\langle x\rangle_0 = (\sigma_0\tau_o/\epsilon_V)/\langle x^{-1}\rangle_1, \quad \text{(A.11)}$$

and

$$(\epsilon_{C_0})_1 = (\sigma_0\tau_o/\epsilon_V)\langle x\rangle_1. \quad \text{(A.12)}$$

The second parts of Eqs. (A.10) and (A.11), following from the use of Eq. (A.6), only apply when the same parameter values are used in $k = 0$ and $k = 1$ response calculations (e.g. β_{01} and β_1 for the KWW situation) leading to the relation $(\epsilon_{C_\infty})_1 = (\epsilon_{C_0})_0$. Thus, only the first parts of these equations apply for fitting of the same data with both CSD0 and CSD1 models. Furthermore, since $\langle x^{-1}\rangle_0$ is infinite for non-Debye CSD0 models which do not include a transition to Debye response at sufficiently high frequencies (no cutoff effects), only the expression for $(\epsilon_{C_0})_0$ is directly useful in this case [56,57], even though the data may actually include a non-zero ϵ_{C_∞} contribution to ϵ_∞ or $\epsilon_C(\omega)$ is still non-negligible in the high-frequency measured range even when ϵ_{C_∞} is zero.

An equation equivalent to the rightmost part of Eq. (A.10) was first derived by Moynihan and his associates [52,53], but they erroneously used ϵ_{D_∞} in place of the pure CSD quantity $(\epsilon_{C_\infty})_1$. Note that the substitution of the first part of Eq. (A.10) into Eq. (A.8) allows it to be written as

$$M_1(\omega) = [1 - I_0(\omega)]/(\epsilon_{C_\infty})_1, \quad \text{(A.13)}$$

a result equivalent to that found in the original modulus formalism work [53] except for the presence there of ϵ_{D_∞}, or later of ϵ_∞ (e.g. [54,67–69]), instead of $(\epsilon_{C_\infty})_1$. The LEVM program allows CSD1 response to be calculated from either Eq. (A.1) with $k = 1$ and Eq. (A.5) or from Eq. (A.13) for several response models with or without cutoff, but the direct use of Eq. (A.5) is more accurate in the low-frequency region because of the presence of the subtraction in Eq. (A.13). The use of Eq. (A.13) or its MFA form is particularly inappropriate for such $I_0(\omega)$ models as that of Havriliak and Negami and the ZC, ones which involve nonphysical limiting low-frequency response, rendering their results for $M_1(\omega)$ progressively more inaccurate as the frequency diminishes [67,68].

Since the original modulus formalism work [53], which dealt with what is here designated as CSD1 behavior, its version of Eq. (A.10)

$$\epsilon_\infty = (\sigma_0\tau_o/\epsilon_V)\langle x\rangle_0 = (\sigma_0/\epsilon_V)\langle\tau\rangle_0, \quad \text{(A.14)}$$

has been widely used over the years in data analysis to estimate ϵ_∞, τ_o, or $\langle\tau\rangle_0$ when the other quantities were thought to be known. In fact, however, this relation is inappropriate when CSD is present, and it must be replaced by Eq. (A.10) above, and estimates of $(\epsilon_{C_\infty})_1$ and ϵ_∞ must be obtained from data fitting, as in the present work. Preliminary results obtained so far suggest that $(\epsilon_{C_\infty})_1$ depends only weakly on temperature, consistent with the usual close agreement of the activation energy estimates found experimentally for τ_o and ρ_0 [56,57].

Although the Maxwell *dielectric* relaxation time, τ_{DR}, is normally defined for a nondispersive material whose dielectric-level response is of Debye form and may be represented by an ideal resistor and an ideal

capacitor in series, its analog for a non-dispersive conductive system consists of an ideal resistor and capacitor in parallel. The resistor then represents the bulk resistance and the capacitor is associated with ϵ_{C_∞}. This conductive-system relaxation time will be designated as τ_{CR} and satisfies the relation $\epsilon_{D_\infty} = \sigma_0 \tau_{CR}/\epsilon_V$.

Consider now what happens to CSD response as the dispersion goes to zero and the response reaches Debye form. Then $\epsilon_C(\omega)$ becomes just a constant, ϵ_C, and Eqs. (A.9)–(A.11) reduce to $\epsilon_C = \sigma_0 \tau_o/\epsilon_V$. There is no reason to expect that τ_o and τ_{CR} will be the same, and the equation $\epsilon_\infty = \epsilon_C + \epsilon_{D_\infty}$ applies. Even non-dispersive Debye relaxation for a conductive system involves a frequency-independent effective dielectric constant ϵ_C in the region where such response is present. In the high-frequency cutoff region where $\tau_o = \tau_{\min}$, one expects ϵ_C to be small, and it may be less than unity [57].

Now transform a full CSD model, that including the dielectric constant ϵ_x, from the complex conductivity level, $\sigma_T(\omega)$, to the complex dielectric constant level, $\epsilon_T(\omega) = \epsilon'_T - i\epsilon''_T \equiv \sigma_T(\omega)/(i\omega\epsilon_V)$. Since $\sigma_T(\omega) = i\omega\epsilon_V\epsilon_x + \sigma_k(\omega)$ and so $\sigma'_T(\omega) = \sigma'_k(\omega)$, it follows that

$$\epsilon_T(\omega) = [\epsilon_x + \{\sigma''_k(\omega)/(\omega\epsilon_V)\}] - i\sigma'_k(\omega)/(\omega\epsilon_V). \tag{A.15}$$

Then let

$$R_k(\omega) \equiv \omega\epsilon_V(\epsilon'_T(\omega) - \epsilon_x)/(\sigma'_k(\omega) - \sigma_0) = (\sigma''_T(\omega) - \omega\epsilon_V\epsilon_x)/(\sigma'_T(\omega) - \sigma_0), \tag{A.16}$$

where the second form is more directly useful since it involves only $\sigma_T(\omega)$ data values. It follows that for the ZC0 model,

$$R_0(\omega) = \tan\{n_{t0}(\omega)\pi/2\}, \tag{A.17}$$

an analog of the constant-phase-element universal-dielectric-response equation of Jonscher [15, Eq. (50)] since a full ZC0 model reduces to a conductive-system constant-phase element after the subtractions of Eq. (A.16). Here we thus expect n_{t0}, a test estimate, to equal the fractional exponent of the Eq. (6) ZC0, n, for exact ZC0 data over its full range of frequencies.

The analysis of [8] leads to results equivalent to the first form of Eq. (A.16) and to Eq. (A.17) but without the ϵ_V quantities appearing above, appropriate if the epsilons in (A.16) represent dielectric permittivities rather than relative dielectric constants, but they are not used consistently in [8]. Finally, instead of concentrating directly on R_k, it is more instructive and useful to calculate n_{tk} from Eqs. (A.17) and (A.18) as

$$n_{tk} = (2/\pi)\tan^{-1}(R_k), \tag{A.18}$$

and use n_{tk} as a diagnostic tool for assessing the presence of ZC0 PLR behavior. For accurate ZC0 experimental or model data, Eq. (A.18) with $k=0$ should lead to the proper frequency-independent estimate of n, while neither KWW1 nor KWW0 response should yield such a constant n value.

References

[1] D.P. Almond, G.K. Duncan, A.R. West, Solid State Ionics 8 (1983) 159.
[2] W.K. Lee, J.F. Liu, A.S. Nowick, Phys. Rev. Lett. 67 (1991) 1559.
[3] B.S. Lim, A.V. Vaysleyb, A.S. Nowick, Appl. Phys. A 56 (1993) 8.
[4] W.K. Lee, B.S. Lim, J.F. Liu, A.S. Nowick, Solid State Ionics 53–56 (1992) 831.
[5] A.S. Nowick, B.S. Lim, J. Non-Cryst. Sol. 172–174 (1994) 1389.
[6] H. Jam, C.H. Hsieh, J. Non-Cryst. Sol. 172–174 (1994) 1408.
[7] A.S. Nowick, A.V. Vaysleyb, B.S. Lim, J. Appl. Phys. 76 (1994) 4429.
[8] D.L. Sidebottom, P.F. Green, R.K. Brow, Phys. Rev. B 51 (1995) 2770.
[9] A.S. Nowick, A.V. Vaysleyb, W. Liu, Solid State Ionics 105 (1998) 121.
[10] H. Jam, S. Krishnaswami, Solid State Ionics 105 (1998) 129.
[11] A.S. Nowick, A.V. Vaysleyb, I. Kuskovsky, Phys. Rev. B 58 (1998) 8398.
[12] D.L. Sidebottom, J. Non-Cryst. Solids 244 (1999) 223.
[13] A.K. Jonscher, The 'universal' dielectric response, Nature 267 (1977) 673.
[14] A.K. Jonscher, in: The Universal Dielectric Response: A Review of Data their New Interpretation, Chelsea Dielectrics Group, London, 1978.
[15] A.K. Jonscher, Physics of Thin Films 80 (1980) 205, Except for minor additions, this work is identical to that of [14].
[16] A.K. Jonscher, in: Dielectric Relaxation in Solids, Chelsea Dielectrics Press, London, 1983.
[17] A.K. Jonscher, J. Phys. C 6 (1973) L235.
[18] D.P. Almond, A.R. West, Solid State Ionics 11 (1983) 57.

[19] D.P. Almond, C.C. Hunter, A.R. West, J. Mater. Sci. 19 (1984) 3236.
[20] J.R. Macdonald, G.B. Cook, J. Electroanal. Chem. 193 (1985) 57.
[21] S.R. Elliott, Solid State Ionics 27 (1988) 131.
[22] A.S. Nowick, B.S. Lim, A.V. Vaysleyb, J. Non-Cryst. Solids 172–174 (1994) 1243.
[23] A.V. Vaysleyb, Phys. Rev. B 58 (I) (1998) 8407.
[24] K.S. Cole, R.H. Cole, J. Chem. Phys. 9 (1941) 341.
[25] H.P. Schwan, in: J.H. Lawrence, C.A. Tobias (Eds.), Advances in Biological and Medical Physics, Vol. V, 1957, p. 147.
[26] D. Ravaine, J.-L. Souquet, CR Acad. Sci. (Paris) 277C (1973) 489.
[27] J.R. Macdonald (Ed.), Impedance Spectroscopy–Emphasizing Solid Materials and Systems, Wiley-Interscience, New York, 1987, pp. 16–20.
[28] O. Bohnke, S. Ronchetti, D. Mazza, Solid State Ionics 22 (1999) 127.
[29] C. Leon, J. Santamaria, M.A. Paris, J. Sanz, J. Ibarra, L.M. Torres, Phys. Rev. B 56 (I) (1997) 5302.
[30] J.R. Macdonald, Solid State Ionics 13 (1984) 147.
[31] K.L. Deori, A.K. Jonscher, J. Phys. C: Solid State Phys. 12 (1979) L289.
[32] H. Fricke, Phil. Mag. 14 (1932) 310.
[33] M. Pollak, T.H. Geballe, Phys. Rev. 122 (1961) 1742.
[34] B.A. Boukamp, J.R. Macdonald, Solid State Ionics 74 (1994) 85.
[35] J.R. Macdonald, J. Non-Cryst. Solids 197 (1996) 83, G_D in Eq. (A2) should be G_{CD}, essentially the present G_1 quantity.
[36] J.R. Macdonald, J. Non-Cryst. Solids 204 (1996) 309, erratum, Ref. [35].
[37] B.A. Boukamp, J. Electrochem. Soc. 142 (1995) 1885.
[38] J.R. Macdonald, L.D. Potter Jr., Solid State Ionics 23 (1987) 61. The new version, V.7.11, of the extensive LEVM fitting program, may be downloaded at no cost from http://www.physics.unc.edu/~macd/. It includes an extensive manual, executable program, and full source code.
[39] J.R. Macdonald, J. Electroanal. Chem. 307 (1991) 1.
[40] J.R. Macdonald, J. Appl. Phys. 75 (1994) 1059.
[41] J.R. Macdonald, Appl. Phys. A 59 (1994) 181.
[42] J.R. Macdonald, J. Non-Cryst. Solids 210 (1997) 70.
[43] C. Cramer, K. Funke, T. Saatkamp, Phil. Mag. B 71 (1995) 701.
[44] C. Cramer, K. Funke, M. Buscher, A. Happe, T. Saatkamp, D. Wilmer, Phil. Mag. B 71 (1995) 713.
[45] B. Durand, G. Taillades, A. Pradel, M. Ribes, J.C. Badot, N. Belhadj-Tahar, J. Non-Cryst. Solids 172–174 (1994) 306.
[46] M. Cutroni, A. Mandanici, A. Piccolo, C. Tomasi, Phil. Mag. B 71 (1995) 843.
[47] J.R. Macdonald, J. Chem. Phys. 36 (1962) 345.
[48] J.R. Macdonald, J.C. Wang, Solid State Ionics 60 (1993) 319.
[49] J.R. Macdonald, J. Appl. Phys. 82 (1997) 3962.
[50] R. Kohlrausch, Pogg. Ann. Phys. Chem. 91 (2) (1854) 179.
[51] G. Williams, D.C. Watts, Trans. Faraday Soc. 66 (1970) 80.
[52] P.B. Macedo, C.T. Moynihan, R. Bose, Phys. Chem. Glasses 13 (1972) 171.
[53] C.T. Moynihan, L.P. Boesch, N.L. Laberge, Phys. Chem. Glasses 14 (1973) 122.
[54] C.T. Moynihan, J. Non-Cryst. Solids 172–174 (1994) 1395.
[55] D.L. Sidebottom, P.F. Green, R.K. Brow, J. Non-Cryst. Solids 183 (1995) 151, The formula for the complex modulus, M, in this work and in [52], but not in [54], is non-standard.
[56] J.R. Macdonald, J. Non-Cryst. Solids 212 (1997) 95.
[57] J.R. Macdonald, J. Appl. Phys. 84 (1998) 812, The word 'out' in the third line from the bottom of the first column on p. 820 should be 'but'.
[58] J.R. Macdonald, Braz. J. Phys. 27 (1999) 332, This paper may be downloaded in full from http://www.sbf.if.usp.br/WWW_pages/Journals/BJP/Vol.29/index.htm.
[59] D.W. Davidson, R.H. Cole, J. Chem. Phys. 39 (1961) 1417.
[60] J.R. Macdonald, Solid State Ionics 25 (1987) 271.
[61] J.R. Macdonald, J. Appl. Phys. 58 (1985) 1955.
[62] J.C. Dyre, Phys. Lett. A 108 (1985) 457.
[63] J.R. Macdonald, J. Appl. Phys. 65 (1989) 4845.
[64] B. Roling, Solid State Ionics 105 (1998) 185.
[65] J.R. Macdonald, Solid State Ionics 124 (1999) 1.
[66] J.R. Macdonald, J. Appl. Phys. 62 (1987) R51.
[67] C.T. Moynihan, J. Non-Cryst. Solids 203 (1996) 359.
[68] C. Leon, M.L. Lucia, J. Santamaria, M.A. Paris, J. Sanz, A. Varez, Phys. Rev. B 54 (I) (1996) 184.
[69] C.T. Moynihan, Solid State Ionics 105 (1998) 175.